PERGAMON

International Journal of Solids and Structures 38 (2001) 8441–8457

INTERNATIONAL JOURNAL OF SOLIDS and STRUCTURES

www.elsevier.com/locate/ijsolstr

Behaviour of the extensible elastica solution

Anders Magnusson, Matti Ristinmaa *, Christer Ljung

Division of Solid Mechanics, Lund University, Box 118, SE-221 00 Lund, Sweden

Received 7 April 2000

Abstract

The general form of the virtual work expression for the large strain Euler–Bernoulli beam theory is derived using the nominal strain (Biot's) tensor. From the equilibrium equations, derived from the virtual work expression, it turns out that a linear relation between Biot's stress tensor and the (Biot) nominal strain tensor forms the differential equation used to derive the elastica solution. Moreover, in the differential equation one additional term enters which is related to the extensibility of the beam axis. As a special application, the well-known problem of an axially loaded beam is analysed. Due to the extensibility of the beam axis, it is shown that the buckling load of the extensible elastica solution depends on the slenderness, and it is of interest that for small slenderness the bifurcation point becomes unstable. This means the bifurcation point changes from being supercritical, which always hold for the inextensible case, i.e. the classical elastica solution, to being a subcritical point. In addition, higher order singularities are found as well as nonbifurcating (isolated) branches.

Keywords: Stability; Elastica; Bifurcation

1. Introduction

The classical problem of buckling of an elastic rod, or beam, under the action of a compressive force will be examined. This is the elastica problem which was analysed already by Bernoulli and Euler, and a thorough discussion of the development of the theory of slender rods can be found in Truesdell (1960), cf. also Antman (1972). A treatment of the global buckling problem for the classical, inextensible, elastica can be found in Love (1927) and Timoshenko and Gere (1961) and a more focused discussion can be found in Reiss (1969).

The difference between the problem studied in the present paper and the classical problem of the elastica is that here the neutral axis is allowed to be extensible. This leads to an additional term in the resulting differential equation compared to the classical case. In Antman and Rosenfeld (1978) an extensive treatment of the global behaviour of buckled states of rods is made. This study is extended in Antman and Pierce (1990) to include nonbifurcating branches. In both these papers the global qualitative properties of bifurcating branches have been studied. In the present paper, however, also quantitative results for the

* Corresponding author. Fax: +46-46-222-4620.
E-mail address: matti.ristinmaa@solid.lth.se (M. Ristinmaa).

0020-7683/01/$ - see front matter
PII: S0020-7683(01)00089-0

pinned–pinned axially loaded beam will be obtained, that shows several of the characteristic qualitative properties predicted in Antman and Rosenfeld (1978) and Antman and Pierce (1990).

When the buckling and postbuckling behaviour of beams are going to be examined, the beam theories of Euler–Bernoulli and Timoshenko for small displacements need to be extended in order to correctly account for effects of large deformations and finite strains. A planar beam theory where the geometrical nonlinearities are precisely taken into account, which can be viewed as a generalization of the Timoshenko beam theory, was presented by Reissner (1972). The Euler–Bernoulli beam, generalized to large deformations, can be obtained from the Reissner beam theory by requiring the shear strain to be zero. The plane beam theory of Reissner was later extended to three dimensions in Reissner (1973), Simo (1985) and Simo and Vu-Quoc (1986).

The governing equations for these beam theories become highly nonlinear. For practical purposes, these kinds of problems are usually solved by some numerical method, e.g. the finite element method. However, to be able to verify the accuracy of the approximate methods, closed-form solutions to problems of this kind are still important. In some cases, closed-form solutions can be obtained for the elastica problems by using elliptic integrals. In Goto et al. (1987, 1990) closed-form solutions with elliptic integrals are found for the extensible elastica and the first buckling mode for a cantilever beam is studied. Closed-form solutions, in terms of elliptic integrals, of the extensible elastic has also been considered by Pflüger (1964).

In the present article, a general treatment of the Euler–Bernoulli beam theory is first made. The governing equations are obtained from the virtual work expression. The linearized problem is then considered, from which the buckling loads for the pinned–pinned beam under an axial compressive force are obtained. It turns out that, in contrast to the classical inextensible elastica, only a limited number of buckling loads exist. Also, the same buckling mode exists at two different buckling loads.

The postbuckling behaviour of the extensible elastica solution is then studied. Closed-form expressions are obtained with elliptic integrals. These are integrated to obtain the postbuckling behaviour of the beam and the shape of the buckled beam.

2. Kinematics and strain tensor for a plane beam

To begin with the assumptions or approximations adopted for the kinematics has to be introduced. First, it is assumed that Euler–Bernoulli's hypothesis is valid, i.e. plane cross-sections, which are perpendicular to the neutral axis before deformation remain plane and perpendicular to the neutral axis after deformation. Next, it is also assumed that the plane cross-sections do not change their shape and area. In Fig. 1 the kinematics of the beam are given when Euler–Bernoulli's hypothesis is assumed to be valid. The deformation of the beam is also restricted to be in the same plane as the undeformed beam occupies, i.e. $\mathbf{e}_1\mathbf{e}_2$-plane.

Each point in the undeformed configuration is identified by its material coordinates x^0, y^0. Making use of Fig. 1 and the assumptions above it can be seen that the displacement components can be written as

$$\begin{aligned} u_1(x^0, y^0) &= u(x^0) - y^0 \sin\theta(x^0), \\ u_2(x^0, y^0) &= w(x^0) - y^0(1 - \cos\theta(x^0)). \end{aligned} \tag{1}$$

Here three new functions have been introduced, $u(x^0)$ and $w(x^0)$, the displacement of the beam axis in the $\mathbf{e}_1$ and $\mathbf{e}_2$ directions, respectively, and $\theta(x^0)$, the rotation of the cross-section. Note that for the Euler–Bernoulli hypothesis θ is the rotation of the neutral axis; the implication of this will be discussed later on. Here, as well as in the proceeding text, all components will refer to the Cartesian base vectors defined in Fig. 1. Moreover, it is noted already here, that the three functions u, w and θ are not independent when the Euler–Bernoulli hypothesis is used, whereas in the Timoshenko hypothesis, where shear strain exists, three

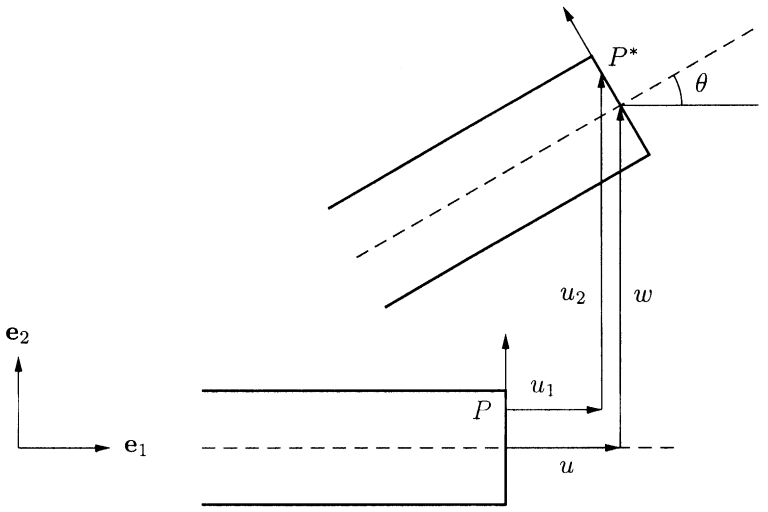

Fig. 1. Illustration of the deformation of a beam cross-section.

independent functions would be used to define the displacement components. If the Timoshenko hypothesis is adopted, Reissner's beam theory is obtained, cf. Reissner (1972, 1981). See also Simo (1985); Simo and Vu-Quoc (1986).

Before entering the discussion about strain tensors, some useful results will be derived. From the deformation of the beam axis it is seen that

$$\sin\theta = \frac{1}{\Lambda + 1}\frac{\mathrm{d}w}{\mathrm{d}x^0} \tag{2}$$

and

$$\cos\theta = \frac{1}{\Lambda + 1}\left(1 + \frac{\mathrm{d}u}{\mathrm{d}x^0}\right), \tag{3}$$

where

$$\Lambda = \sqrt{\left(1 + \frac{\mathrm{d}u}{\mathrm{d}x^0}\right)^2 + \left(\frac{\mathrm{d}w}{\mathrm{d}x^0}\right)^2} - 1. \tag{4}$$

These follow directly from geometrical considerations. Note that these relations hold in general and are not related to the Euler–Bernoulli hypothesis. From Eqs. (2) and (3) it is clear that $u(x^0)$, $w(x^0)$ and $\theta(x^0)$ cannot be independent of each other. This will cause some problems that will have to be dealt with later on.

Before the virtual work can be established, some consideration about the strain tensor is needed. It is well known that many different strain tensors exist. Thus the question arises, which strain tensor should be used? Obviously any of the strain tensors could be used and there is no definite way to make the selection based on theory alone; but since the goal here is to derive the elastica solution it turns out that a natural choice, as will be shown, is the Biot or nominal strain tensor.

The nominal strain tensor, $\mathbf{E}^{(1)}$, is defined as

$$\mathbf{E}^{(1)} = \mathbf{U} - \mathbf{I}, \tag{5}$$

where $\mathbf{I}$ is the second order identity tensor and $\mathbf{U}$ the right stretch tensor defined as $\mathbf{U} = (\mathbf{F}^{\mathrm{T}}\mathbf{F})^{1/2}$, where $\mathbf{F}$ is the deformation gradient. The superscript (1) indicates that $\mathbf{E}^{(1)}$ is linear in the stretches.

From $\mathbf{U} = (\mathbf{F}^{\mathrm{T}}\mathbf{F})^{1/2}$, the definition of the deformation gradient and taking advantage of Eqs. (2)–(4) it follows that only one strain component exists, the normal strain in the $\mathbf{e}_1$-direction, i.e.

$$E^{(1)} = \Lambda - y^0 K, \tag{6}$$

where

$$K = \frac{\mathrm{d}\theta}{\mathrm{d}x^0} \tag{7}$$

has been introduced.

3. Virtual work

After this introduction it is now time to establish the virtual work expression. The virtual work expression for static loading situations, described in terms of the nominal strains, $E_{ij}^{(1)}$, and (symmetrized) Biot's stresses (sometimes referred to as Jaumann's stress tensor), $S_{ij}^{(1)}$ is used as the starting point, cf. Atluri and Cazzani (1995). To obtain the relevant virtual work expression for the beam, the geometry of the beam and the kinematic assumptions discussed previously, must be introduced. It then follows that the virtual work expression for the beam can be written as

$$\int_{x^0} (\delta\Lambda N - \delta K M)\,\mathrm{d}x^0 = \int_{x^0} (\delta u\, q_x + \delta w\, q_y - \delta\theta\, m)\,\mathrm{d}x^0 + [\delta u F + \delta w Q - \delta\theta M_{\mathrm{b}}]_0^L, \tag{8}$$

where the two cross-section resultants normal force N and the moment M are defined in standard fashion. Moreover, q_x, q_y and m denote the distributed loads, in the x^0- and y^0-directions, and moment per unit length, respectively. Finally, F, Q and M_{b} are the applied end normal force, shear force and moment, respectively.

In the above virtual work, apart from the Euler–Bernoulli assumptions, no approximations have been made and the virtual work expression above therefore holds for a beam capable of undergoing large deformations as well as large rotations. Note that the kinematic assumption is the only "approximation" used to derive Eq. (8), therefore, it is sometimes referred to as a kinematically or geometrically exact theory.

It turns out that it is necessary to be very careful when dealing with Eq. (8). As previously mentioned there are only two independent functions, whereas Eq. (8) contains three functions, u, w and θ. Thus the variation of the three functions in Eq. (8) are not independent.

It can be noted that if $q_y = 0$ as well as $Q = 0$ then a formulation in u and θ can be obtained. To eliminate δw in Eq. (8), the variation of Eqs. (2) and (3) is used to obtain

$$\delta\Lambda = \frac{1}{\cos\theta}\frac{\mathrm{d}\delta u}{\mathrm{d}x^0} + (\Lambda + 1)\tan\theta\,\delta\theta.$$

It then follows that the virtual work expression (8) can be written as

$$\int_{x^0} \left(\frac{\mathrm{d}\delta u}{\mathrm{d}x^0}\frac{1}{\cos\theta} + \delta\theta(\Lambda + 1)\tan\theta\right) N\mathrm{d}x^0 - \int_{x^0} \frac{\mathrm{d}\delta\theta}{\mathrm{d}x^0} M\mathrm{d}x^0 = \int_{x^0} (\delta u\, q_x - \delta\theta\, m)\mathrm{d}x^0 + [\delta u F - \delta\theta M_{\mathrm{b}}]_a^b. \tag{9}$$

Finally, by letting $q_x = m = 0$ and $M_{\mathrm{b}} = 0$ at the end points, the virtual work expression can be used to obtain the equilibrium equations for an axially loaded beam as

$$N = F\cos\theta, \tag{10a}$$

$$\frac{\mathrm{d}M}{\mathrm{d}x^0} + (\Lambda + 1)F\sin\theta = 0. \tag{10b}$$

Thus, the simplest form of the equilibrium equation applicable for an Euler–Bernoulli beam has obtained, if the pure bending situation is excluded.

3.1. Equilibrium equations for an axially loaded beam

In order to be able to express the equilibrium equations (10a) and (10b) in terms of displacements and rotations, the resultant forces N and M have to be expressed in these quantities. If a linear relation between Biot stress and nominal strain, $S^{(1)} = EE^{(1)}$, where E is Young's modulus, is assumed, the resultant forces can be rewritten from their definitions, with use of Eq. (6), as

$$M = -EI^0\frac{\mathrm{d}\theta}{\mathrm{d}x^0}, \tag{11a}$$

$$N = EA^0\Lambda, \tag{11b}$$

where I^0 and A^0 denote the moment of inertia and the cross-section area, respectively. It should be noted that by adopting a linear relation between the stress and the strain, the constitutive relation between the normal force N and the quantity Λ in Eq. (11b) does not have the desired property that $N \to -\infty$ as $\Lambda \to -1$ (see e.g. Antman and Rosenfeld, 1978). The consequence of not fulfilling this is that there will be a nonadmissible region which would correspond to the beam being pushed through itself. One possible form of constitutive model for the normal force that has the desired properties when Λ approaches -1 is given by (cf. Antman and Pierce, 1990),

$$N = \frac{EA^0}{1+\gamma}\left(\Lambda + 1 - \frac{1}{(\Lambda+1)^\gamma}\right), \tag{12}$$

where $\gamma > 0$. For Λ close to zero, N will be proportional to Λ, i.e. $N = EA^0\Lambda + \mathrm{O}(\Lambda^2)$, cf. Eq. (11b). It can also be seen that in the limit where $\gamma \to 0$, Eq. (12) approaches Eq. (11b), so that for small exponents γ, the linear relationship between N and Λ is obtained, except very close to $\Lambda = -1$, where N approaches $-\infty$. It can thus be argued that instead of using Eq. (12) with a small exponent γ, the simpler linear relation (11b) could be used. However, the results should not be considered as mechanically reliable when Λ is close to -1. This is indeed the approach chosen here, which has the consequence that there are nonadmissible regions, where $\Lambda \leqslant -1$, in the figures to come. This material model, i.e. Eq. (11b) and the condition that $\Lambda > -1$, corresponds to a "spring-like" material, which is linear until the spring is compressed to its end position where it suddenly becomes very stiff. It could be realized by a foam material which behaves linearly until all the voids have collapsed, after which it becomes very stiff.

Assuming that a compressive force exists, i.e. $F = -P$ at the ends of the beam, it follows that the boundary term in the axial direction is given as

$$\frac{N}{\cos\theta} = F = -P. \tag{13}$$

Moreover, using Eqs. (11a) and (11b) it follows that

$$\Lambda = -\frac{P}{EA^0}\cos\theta \tag{14}$$

and Eq. (10b) can then be written as

$$EI^0\frac{\mathrm{d}^2\theta}{\mathrm{d}x^{0^2}}+P\sin\theta-\frac{P^2}{EA^0}\cos\theta\sin\theta=0. \tag{15}$$

It can be noted from the results in Antman and Rosenfeld (1978) that if shear deformations were allowed, an additional term, $\eta P\cos\theta$, would enter the equilibrium equation (15), where η is a shear type of strain. Here it is assumed that no shearing occurs, which corresponds to setting $\eta=0$. Thus the equilibrium equation for the axially loaded beam in terms of kinematic quantities have been found. In fact, the above equation will serve as the starting point in the derivation of the extensible elastica solution.

Note that the last term, appearing in Eq. (15), is usually not present in the literature, since it disappears using the classical inextensibility assumption, which corresponds to $\Lambda=0$, i.e. no extension of the beam axis. It was, however, included by Pflüger (1964) who also proceeded to solve Eq. (15).

For completeness the potential energy, U, for the axially loaded beam is derived. Assume that $u(0)=0$ and that a compressive load, P, is applied at $x=L$. A straightforward calculation reveals that the potential energy then takes the form

$$U=\frac{1}{2}EI^0\int_0^L\left(\frac{\mathrm{d}\theta}{\mathrm{d}x^0}\right)^2\mathrm{d}x^0+\frac{1}{2}EA^0\int_0^L\Lambda^2\,\mathrm{d}x^0+Pu(L), \tag{16}$$

where the second term corresponds to the extensibility of the beam axis. Moreover, by using

$$u(L)=\int_0^L\frac{\mathrm{d}u}{\mathrm{d}x^0}\,\mathrm{d}x^0=\int_0^L[(\Lambda+1)\cos\theta-1]\,\mathrm{d}x^0$$

and Eq. (14), it is clear that Eq. (16) can be written as

$$U=\frac{1}{2}EI^0\int_0^L\left(\frac{\mathrm{d}\theta}{\mathrm{d}x^0}\right)^2\mathrm{d}x^0-\frac{P^2}{2EA^0}\int_0^L\cos^2\theta\,\mathrm{d}x^0+P\int_0^L(\cos\theta-1)\,\mathrm{d}x^0. \tag{17}$$

In fact, Eq. (17) will be used when the properties of the elastica solution are examined.

4. The extensible elastica solution

With the tools of the previous section, it is now possible to derive the well-known closed–form solution – the elastica – to the large displacement version of the pinned–pinned column subjected to a compressive axial load, cf. Fig. 2. The starting point is of course the equilibrium equation (15) for the beam together with the end conditions of a pinned–pinned beam: the transverse displacements and moments are zero at the ends of the beam and the longitudinal displacement is zero at the left end.

$$w=0\quad\text{and}\quad M=EI^0\frac{\mathrm{d}\theta}{\mathrm{d}x^0}=0\text{ at }x^0=0\quad\text{and}\quad x^0=L,\quad\text{and}\quad u=0\text{ at }x^0=0. \tag{18}$$

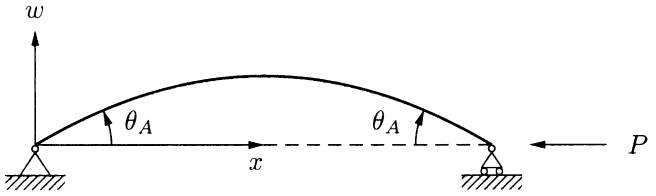

Fig. 2. A pinned–pinned beam under external load consisting of an axial compressive force P.

The goal is to find a slope $\theta(x^0)$ such that it corresponds to an equilibrium deformed position of the column under the action of the axial load P. Once this slope is found, Eq. (2) can be used to compute the transverse displacements and Eq. (3) to compute the axial displacements. From the elementary treatment of the problem it is not expected to find a nonzero solution for axial loads below the Euler load

$$P_{\mathrm{E}} = \pi^2 \frac{EI^0}{L^2}. \tag{19}$$

To summarize, the problem is defined by the ordinary differential equation (15) which has to be solved under observation of the boundary conditions

$$\left.\frac{\mathrm{d}\theta}{\mathrm{d}x^0}\right|_{x^0=0} = \left.\frac{\mathrm{d}\theta}{\mathrm{d}x^0}\right|_{x^0=L} = 0 \tag{20}$$

obtained from Eq. (18). It can be noticed that a trivial solution $\theta = 0$ exists, i.e. the fundamental solution, however what is interesting here is to find a nontrivial solution corresponding to a deformed equilibrium position of the column. Moreover, it follows from the boundary conditions and the equilibrium equation that reflectional symmetry or $\mathbf{Z}_2$-symmetry exists in the problem description.

4.1. Linearized problem

Before the delicate discussion about the elastica problem is entered, the properties of the fundamental solution are analysed. It turns out that it is sufficient to consider the linearized problem around $\theta = 0$ when the fundamental path is analysed. First the eigenvalue problem is considered. A linearization of Eq. (15) yields

$$EI^0 \frac{\mathrm{d}^2\theta}{\mathrm{d}x^{0_2}} + \left(P_{\mathrm{cr}} - \frac{P_{\mathrm{cr}}^2}{P_{\mathrm{E}}} \frac{\pi^2}{\lambda^2}\right)\theta = 0, \tag{21}$$

where the Euler load (19) and the slenderness

$$\lambda = \sqrt{\frac{A^0 L^2}{I^0}} \tag{22}$$

have been introduced and P_{cr} is the buckling load. It should be noted that the classical inextensible elastica solution is obtained be letting $\lambda \to \infty$.

Note that with the Euler load P_{E} from Eq. (19) and the slenderness λ from Eq. (22), Eq. (14) can be written as

$$\Lambda = -\frac{\pi^2}{\lambda^2} \frac{P}{P_{\mathrm{E}}} \cos\theta. \tag{23}$$

This means that for the fundamental path, i.e. $\theta = 0$, the admissible region, defined by $\Lambda > -1$, cf. the discussion related to Eqs. (11a) and (11b), is obtained as

$$\frac{P}{P_{\mathrm{E}}} < \frac{\lambda^2}{\pi^2}, \tag{24}$$

cf. Fig. 3.

From the eigenvalue problem (21) and the associated boundary conditions Eq. (20) it follows that the eigenfunctions are given as

$$\theta_n = c_n \cos\frac{n\pi x^0}{L}, \quad n = 1, 2, 3 \ldots, \tag{25}$$

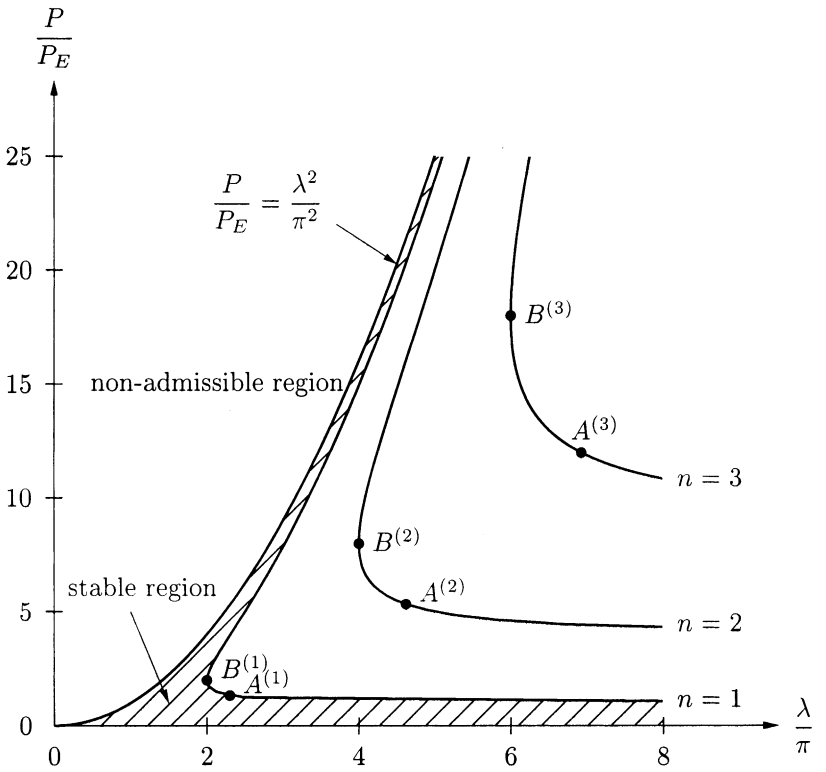

Fig. 3. Buckling load at the fundamental path for the three first modes. Note for $\lambda < 2\pi$ the fundamental path is always stable. The points $A^{(1)}$, $A^{(2)}$, $A^{(3)}$ and $B^{(1)}$, $B^{(2)}$, $B^{(3)}$ mark where the postbuckling branches change curvature.

where the c_n-coefficients are arbitrary. Insertion of Eq. (25) into Eq. (21) yields that

$$\left[- EI^0 \left(\frac{n\pi}{L} \right)^2 + \left(P_{\mathrm{cr}} - \frac{P_{\mathrm{cr}}^2}{P_{\mathrm{E}}} \frac{\pi^2}{\lambda^2} \right) \right] c_n \cos \frac{n\pi x^0}{L} = 0$$

or

$$\left(\frac{P_{\mathrm{cr}}}{P_{\mathrm{E}}} \right)^2 - \frac{P_{\mathrm{cr}}}{P_{\mathrm{E}}} \frac{\lambda^2}{\pi^2} + n^2 \frac{\lambda^2}{\pi^2} = 0 \tag{26}$$

must hold in general. The solution to this second-order equation is given by

$$\frac{P_{\mathrm{cr}}}{P_{\mathrm{E}}} = \frac{\lambda^2}{2\pi^2} \pm \sqrt{\frac{\lambda^4}{4\pi^4} - n^2 \frac{\lambda^2}{\pi^2}}. \tag{27}$$

In Fig. 3 the dependency of the buckling load on the slenderness is shown. It is of interest that for the classical inextensible elastica, where $\lambda \to \infty$ holds, Eq. (26) implies that infinitely many buckling loads exist, with the buckling load given by

$$P_{\mathrm{cr}}^{\mathrm{in}} = n^2 P_{\mathrm{E}}.$$

In contrast, Eq. (27) shows that for the extensible elastic only a limited number of buckling loads exist. Moreover, if the case $n = 1$ and $\lambda = 3\pi$ is considered, it turns out that there exist two buckling loads with

the same eigenmode, and for $\lambda = 5\pi$ a total of four buckling loads belonging to two different eigenmodes, $n = 1$ and 2, exist. From Eq. (27) it follows that $\lambda > 2\pi n$ if real solutions are expected. For $\lambda < 2\pi$ it then follows that no real eigenvalues (buckling loads) exist on the fundamental path, implying that no branches emerge. A physical interpretation of this could be that the shortening of the beam compensates the increase of the load that much that buckling never occurs. Finally, it can be noted that $\lambda = 2\pi$ corresponds to a double root for the first mode at point $B^{(1)}$, so does $\lambda = 4\pi$ for the second mode at point $B^{(2)}$. The implication of these aspects will be discussed more in detail when the elastica solution is considered. Moreover, for the extensible beam, it is also observed that the buckling load, P_{cr}, is always higher than for the inextensible case, i.e. for the first mode we find

$$\frac{P_{\mathrm{cr}}}{P_{\mathrm{E}}} = \left(1 + \frac{\pi^2}{\lambda^2} + \mathrm{O}\left(\frac{\pi^4}{\lambda^4}\right)\right).$$

The stability properties of the fundamental solution can be obtained from the potential function, cf. Eq. (17), by considering the second variation of the potential energy, i.e.

$$\delta^2 U = EI^0 \int_0^L \left(\frac{\mathrm{d}\delta\theta}{\mathrm{d}x^0}\right)^2 \mathrm{d}x^0 + \frac{P^2}{EA^0} \int_0^L [\cos^2\theta - \sin^2\theta]\,\delta\theta^2\,\mathrm{d}x^0 - P\int_0^L \cos\theta\,\delta\theta^2\,\mathrm{d}x^0.$$

Linearization around $\theta = 0$ yields

$$\delta^2 U = EI^0 \int_0^L \left(\frac{\mathrm{d}\delta\theta}{\mathrm{d}x^0}\right)^2 \mathrm{d}x^0 + \frac{P^2}{EA^0} \int_0^L \delta\theta^2\,\mathrm{d}x^0 - P\int_0^L \delta\theta^2\,\mathrm{d}x^0.$$

Note that the first variation of the potential function could also have been used for our eigenvalue problem leading to the eigenfunctions (25) and buckling loads (27). Using that

$$\delta\theta = \delta c_n \cos\frac{n\pi x^0}{L},$$

the second variation of the potential can be written

$$\delta^2 U = \left[EI^0\left(\frac{n\pi}{L}\right)^2 + \frac{P^2}{EA^0} - P\right](\delta c_n)^2\frac{L}{2}.$$

For a stable system it is required that $\delta^2 U > 0$, i.e.

$$n^2\frac{\lambda^2}{\pi^2} + \left(\frac{P}{P_{\mathrm{E}}}\right)^2 - \frac{P}{P_{\mathrm{E}}}\frac{\lambda^2}{\pi^2} > 0. \tag{28}$$

The stability region is shown in Fig. 3, and it appears that for $\lambda < 2\pi$ the fundamental solution is stable for all values of P/P_{E}. An interesting observation from Eq. (28) is that for high values of P/P_{E} the system becomes stable, but it should be noted that this state is close to the nonadmissible region.

4.2. Neighbourhood of the singular points

Let us now consider the properties of the bifurcation points in a more general setting such that the corresponding normal forms and codimensions can be found. To realize this the nonlinear terms in the equilibrium equation (15) are expanded in a Taylor series around $\theta(x^0) = 0$ such that

$$\frac{L^2}{\pi^2}\frac{\mathrm{d}^2\theta}{\mathrm{d}x^{02}} + \left(\frac{P}{P_{\mathrm{E}}} - \left(\frac{P}{P_{\mathrm{E}}}\frac{\pi}{\lambda}\right)^2\right)\theta - \left(\frac{1}{6}\frac{P}{P_{\mathrm{E}}} - \frac{2}{3}\left(\frac{P}{P_{\mathrm{E}}}\frac{\pi}{\lambda}\right)^2\right)\theta^3 + \left(\frac{1}{120}\frac{P}{P_{\mathrm{E}}} - \frac{2}{15}\left(\frac{P}{P_{\mathrm{E}}}\frac{\pi}{\lambda}\right)^2\right)\theta^5 + \mathrm{O}(\theta^7) \tag{29}$$

where use was made of the definitions of the Euler load (19) and the slenderness (22). Next, using the eigenfunctions (25) found in the linearized problem and at the same time introducing the definitions

$$\lambda_{\mathrm{p}} = \frac{1}{2n^2}\frac{P}{P_{\mathrm{E}}}, \quad k = \frac{1}{2n^2}\left(\frac{\lambda}{\pi}\right)^2, \tag{30}$$

allow us to write Eq. (29) as

$$g(\theta_n, \lambda_{\mathrm{p}}) = \left(2\lambda_{\mathrm{p}} - \frac{2}{k}\lambda_{\mathrm{p}}^2 - 1\right)\theta_n - \left(\frac{1}{3}\lambda_{\mathrm{p}} - \frac{4}{3k}\lambda_{\mathrm{p}}^2\right)\theta_n^3 + \left(\frac{1}{60}\lambda_{\mathrm{p}} - \frac{4}{15k}\lambda_{\mathrm{p}}^2\right)\theta_n^5 + \mathrm{O}(\theta_n^7). \tag{31}$$

To conclude, using the eigenfunctions, the continuous system in Eq. (29) can be treated as a discrete system, close to $\theta = 0$, which is described by Eq. (31). Moreover, it is also noted that an identical function g given by Eq. (31) can be obtained by considering a spring-link system, cf. Golubitsky and Schaeffer (1984, p. 245), see also Poston and Stewart (1996, p. 302) for the spring-link system.

The function $g(\theta_n, \lambda_{\mathrm{p}})$ describes the equilibrium curves near $\theta = 0$ in a $\lambda_{\mathrm{p}} - \theta$ graph, i.e. it allows us to examine the behaviour close to the bifurcation points found on the fundamental path. The linear term in Eq. (31) corresponds to the linearized problem treated previously, i.e. the requirement for a bifurcation to occur is that this term vanishes, cf. also Eq. (26). It is also noted that since w is linear in $\mathrm{d}\theta/\mathrm{d}x^0$, as will be show later on cf. Eq. (45), g will also reveal the shape of the equilibrium curves in a $\lambda_{\mathrm{p}} - w$ graph, i.e. the cubic term in Eq. (31) reveals the sign of the initial slope of $\mathrm{d}\lambda_{\mathrm{p}}/\mathrm{d}w$.

Since $g(\theta_n, \lambda_{\mathrm{p}})$ given by Eq. (31) was considered by Golubitsky and Schaeffer (1984) some useful results can be extracted from their analysis. For the points $B^{(i)}$, $i = 1, 2, 3\ldots$, shown in Fig. 3 it was found, previously, that $\lambda = 2\pi n$ which from Eq. (28) then yields $P_{\mathrm{cr}}/P_{\mathrm{E}} = 2n^2$ and using Eq. (30) we obtain $k = 2$ and $\lambda_{\mathrm{p}} = 1$. Golubitsky and Schaeffer (1984) showed that for $k = 2$ and near $\theta_n = 0$ and $\lambda_{\mathrm{p}} = 1$ the normal form is given by $\theta_n^3 - \lambda_{\mathrm{p}}^2\theta_n$ and that g exhibits a nondegenerated cubic singularity, i.e. a singularity of codimension five. However, if $\mathbf{Z}_2$-symmetry is enforced this singularity has codimension one for which the universal unfolding is given by $\theta_n^3 - \lambda_{\mathrm{p}}^2\theta_n + \alpha\theta_n$. In fact, it turns out that this universal unfolding is contained in the model and corresponds to Fig. 6(a)–(c), which are derived later on from the exact elastica solution (see also Golubitsky and Schaeffer, 1984, p. 268).

It also turns out that the normal form $\theta_n^3 + \lambda_{\mathrm{p}}^2\theta_n$ cannot be found in the present model, i.e. the isola bifurcation will not be found. However, one would expect, based on the nonlinear spring-link model treated in Troger and Steindl (1991, p. 294), that this normal form can be obtained if nonlinear constitutive relations are adopted instead of the linear one given by Eqs. (11a) and (11b). The formation of isola bifurcations was in fact obtained by Antman and Pierce (1990) for a more general constitutive relation.

The points $A^{(i)}$, $i = 1, 2, 3\ldots$, shown in Fig. 3 are characterized by the fact that the cubic term in Eq. (31) vanishes, i.e. the slope $\mathrm{d}\lambda_{\mathrm{p}}/\mathrm{d}w$ changes sign at these points. This will occur for $k = 8/3$ which corresponds to $(\lambda/\pi)^2 = 16n^2/3$ and the bifurcation load $\lambda_{\mathrm{p}} = 2/3$ corresponding to $P_{\mathrm{cr}}/P_{\mathrm{E}} = 4/3n^2$. Note that this bifurcation load corresponds to the lower load obtained by Eq. (27). Following once more the analysis of Golubitsky and Schaeffer (1984) it is concluded that the normal form is given by $-\theta_n^5 + \lambda_{\mathrm{p}}\theta_n$ which has the codimension four. As previously, if $\mathbf{Z}_2$-symmetry is enforced, this singularity has codimension one for which the universal unfolding is given by $-\theta_n^5 + \lambda_{\mathrm{p}}\theta_n + \alpha\theta_n$. It turns out that this universal unfolding is also contained in the model and is shown in Fig. 7 (see also Golubitsky and Schaeffer, 1984, p. 268). From the λ_{p}–w graph or P/P_{E}–w graph it can then be concluded that the usual bifurcation, supercritical, found in the inextensible elastic can in fact become subcritical and the parametric point where this occurs is given by

$$\frac{P_{\mathrm{cr}}}{P_{\mathrm{E}}} = \frac{4}{3}n^2 \quad \text{and} \quad \lambda_{\mathrm{cr}} = \frac{4}{\sqrt{3}}\pi n. \tag{32}$$

Finally, if $k > 2$ and $k \neq 8/3$ it can be shown that the normal form is given by $\theta_n^3 - \lambda_p \theta_n$, i.e. the usual pitchfork bifurcation found in the inextensible elastic is obtained, with codimension two and codimension zero if $\mathbf{Z}_2$-symmetry is enforced.

For the upper buckling load, which can be solved from Eq. (27) or by requiring that the linear term in Eq. (31) vanishes identically, it follows that the cubic term will always have the same sign for $k > 2$, i.e. the bifurcation point will have the same characteristic for all $k > 2$.

4.3. Equilibrium paths

Eq. (15), although harmless in appearance, is in fact rather difficult to solve because of the nonlinearity inherent in the terms $\sin\theta$ and $\sin\theta\cos\theta$. However, it will be shown that it is possible obtain an implicit solution in terms of elliptic integrals. First, Eq. (15) is multiplied by $\mathrm{d}\theta/\mathrm{d}x^0$, so that it becomes

$$EI^0 \frac{\mathrm{d}\theta}{\mathrm{d}x^0} \frac{\mathrm{d}^2\theta}{\mathrm{d}x^{0_2}} + P\sin\theta \frac{\mathrm{d}\theta}{\mathrm{d}x^0} - \frac{P^2}{EA^0}\cos\theta\sin\theta\frac{\mathrm{d}\theta}{\mathrm{d}x^0} = 0, \tag{33}$$

which can be written as

$$\frac{\mathrm{d}}{\mathrm{d}x^0}\left[\frac{1}{2}EI^0\left(\frac{\mathrm{d}\theta}{\mathrm{d}x^0}\right)^2 - P\cos\theta + \frac{P^2}{2EA^0}\cos^2\theta\right] = 0. \tag{34}$$

The last expression is immediately integrable.

At the ends of a pinned column, θ is unknown, whereas $\mathrm{d}\theta/\mathrm{d}x^0 = 0$ according to Eq. (20). Integration of Eq. (34) and letting α be the unknown slope at the column ends, it follows that

$$\frac{1}{2}EI^0\left(\frac{\mathrm{d}\theta}{\mathrm{d}x^0}\right)^2 = P\cos\theta - \frac{P^2}{2EA^0}\cos^2\theta - P\cos\alpha + \frac{P^2}{2EA^0}\cos^2\alpha. \tag{35}$$

Hence,

$$\frac{\mathrm{d}\theta}{\mathrm{d}x^0} = \frac{2\pi}{L}\sqrt{\frac{P}{P_E}}\sqrt{(1-e)\left(q^2 - \sin^2\frac{\theta}{2}\right) + e\left(q^4 - \sin^4\frac{\theta}{2}\right)}, \tag{36}$$

where the positive root was chosen and definition of the Euler load (19) was used. Moreover, the extensibility parameter e was introduced according to

$$e = \frac{P}{EA^0} = \frac{\pi^2}{\lambda^2}\frac{P}{P_E} \tag{37a}$$

and

$$q = \sin\frac{\alpha}{2}. \tag{37b}$$

As previously mentioned, the classical inextensible case occurs when $\lambda \to \infty$, i.e. when $e \to 0$. For an analogy between Eq. (35) and the oscillating pendulum the reader should consult Love (1927, p. 402) or Antman and Rosenfeld (1978).

In order to simplify the notation, a new variable ϕ is introduced, defined by

$$\sin\frac{\theta}{2} = \sin\frac{\alpha}{2}\sin\phi = q\sin\phi. \tag{38}$$

This new variable will by used as a substitution for θ, the slope of the beam, and it is immediately clear that if Eq. (36) can be solved for ϕ and q, the slope can be calculated using Eq. (38). Since it is known that θ will

have $n+1$ extreme values, cf. Eq. (25), where two extreme values $\pm\alpha$ are found at the ends of the beam, the new variable ϕ is expected to vary from $-\pi/2$ to $n\pi-\pi/2$ from one end of the beam to the other according to the definition (38). Introducing the substitution Eq. (38) into Eq. (36) gives

$$\frac{\mathrm{d}\theta}{\mathrm{d}x^0}=\frac{\mathrm{d}\phi}{\mathrm{d}x^0}\frac{\mathrm{d}\theta}{\mathrm{d}\phi}=\frac{2\pi}{L}\sqrt{\frac{P}{P_{\mathrm{E}}}}(q\cos\phi)\sqrt{1-e+q^2e(1+\sin^2\phi)}. \tag{39}$$

Differentiating Eq. (38) and rearranging the result leads to

$$\frac{\mathrm{d}\theta}{\mathrm{d}\phi}=\frac{2q\cos\phi}{\sqrt{1-q^2\sin^2\phi}}, \tag{40}$$

which, when combined with Eq. (39), yields

$$\frac{\mathrm{d}\phi}{\mathrm{d}x^0}=\frac{\pi}{L}\sqrt{\frac{P}{P_{\mathrm{E}}}}\sqrt{1-q^2\sin^2\phi}\sqrt{1-e+q^2e(1+\sin^2\phi)}, \tag{41}$$

which can be implicitly integrated to yield

$$\int_0^{\pi/2}\frac{\mathrm{d}\phi}{\sqrt{1-q^2\sin^2\phi}\sqrt{1-e+q^2e(1+\sin^2\phi)}}=\frac{\pi}{2n}\sqrt{\frac{P}{P_{\mathrm{E}}}}, \tag{42}$$

where the periodicity of $\sin^2\phi$ was used.

The integral on the left side of Eq. (42) can be reduced to an elliptic integral on Legendre's normal form through the substitution of variables

$$\sin^2\phi=\frac{(1-e+eq^2)\sin^2\psi}{1-e+2eq^2-eq^2\sin^2\psi}$$

following Gröbner and Hofreiter (1961). It is straightforward to show that this transformation is invertible, i.e. it defines a one-to-one relationship between ϕ and ψ, is $e\leqslant 1$. With this substitution and the definitions (37a) and (37b), Eq. (42) becomes

$$\begin{aligned}\frac{\pi}{2}\sqrt{\frac{P}{P_{\mathrm{E}}}}=\frac{\lambda\sqrt{e}}{2}&=\int_0^{\pi/2}\frac{n\,\mathrm{d}\psi}{\sqrt{1-e+2eq^2-q^2(1+eq^2)\sin^2\psi}}\\&=\frac{n}{\sqrt{1-e+2eq^2}}K\left(q\sqrt{\frac{1+eq^2}{1-e+2eq^2}}\right).\end{aligned} \tag{43}$$

The integral in Eq. (43) is a complete elliptic integral of the first kind, $K(k)$, and its values are tabulated in e.g. Abramowitz and Stegun (1970). Especially it is found that $K(0)=\pi/2$, and since this occurs when $q=0$, which in turn means that the beam end-point slopes vanish, it is found that Eq. (43) degenerates to Eq. (26), i.e. an equation from which the buckling loads can be calculated is obtained. An equivalent solution was obtained by Pflüger(1964) through a sequence of variable substitutions of similar nature to the ones used above. However, Pflüger (1964) only discussed the properties of the solution for small values of slope.

To recapitulate what has been achieved so far, from Eq. (43) a matching pair e and q can be calculated for a given slenderness λ. From Eqs. (37a) and (37b) the corresponding load P/P_{E} is then found. Note that Eq. (43) forms a nonlinear equation system and must be solved in an iterative manner. In the calculations, after a start value was obtained, an arc-length method was utilised in the eq-plane to obtain the graphs in

this article. It turns out that the maximum transverse deflection $w_{\max}$ can be computed quite easily in terms of P/P_E. Note from Eq. (2) that $(\Lambda + 1)\sin\theta = \mathrm{d}w/\mathrm{d}x^0$, so that the differential equation (15) can be written

$$EI^0 \frac{\mathrm{d}^2\theta}{\mathrm{d}x^{0_2}} + P\frac{\mathrm{d}w}{\mathrm{d}x^0} = 0, \tag{44}$$

which in turn can be integrated,

$$w = -\frac{EI^0}{P}\frac{\mathrm{d}\theta}{\mathrm{d}x^0} + c_2. \tag{45}$$

At the column ends, both the deflection and the moment vanish, so that $c_2 = 0$. From Eq. (36) it is possible to solve $\mathrm{d}\theta/\mathrm{d}x^0$, giving

$$w = -2\sqrt{\frac{EI^0}{P}}\sqrt{(1-e)\left(q^2 - \sin^2\frac{\theta}{2}\right) + e\left(q^4 - \sin^4\frac{\theta}{2}\right)}. \tag{46}$$

The maximum deflection occurs at $\theta = 0$, so that

$$w_{\max} \equiv \max|w| = 2\sqrt{\frac{EI^0}{P}}\sqrt{(1-e)q^2 + eq^4}, \tag{47}$$

which can easily be brought into the form

$$\frac{w_{\max}}{L} = \frac{2}{\pi}\sqrt{\frac{P_E}{P}}\sqrt{(1-e)q^2 + eq^4}. \tag{48}$$

Now it is possible to plot the load–deflection curves, i.e. P/P_E against $w_{\max}/L$, using Eq. (43) to compute the pair e and q for a given λ and Eq. (37a) to obtain P/P_E, and then Eq. (48) to compute $w_{\max}/L$ given q and P/P_E.

To obtain the shape of the beam, Eq. (36) is integrated for given P/P_E and q with integration limits $\pm 2\sin^{-1}(q)$ to θ. To obtain the transversal deflection Eq. (46) can then be used. For the longitudinal deflection use can be made of Eq. (3). The results for the first three modes are shown for the classical elastica in Fig. 4, where the shape of the beam has been calculated for the slopes $\alpha = \pi/4$ and $\alpha = 3\pi/4$. For a more complete exposition of the mode shapes the reader should consult Love (1927). In fact, it turns out that the mode shape for the extensible elastica has the same form as the classical inextensible elastica, although the length is changed.

For a slender beam, with a high value of the slenderness λ, it would be sensible to use the approximation $e = 0$, cf. Eq. (37a). For completeness the classical elastica solution where $e = 0$ will therefore be considered. With $e = 0$, Eq. (43) becomes

$$\sqrt{\frac{P}{P_E}} = \frac{2n}{\pi}\int_0^{\pi/2}\frac{\mathrm{d}\psi}{\sqrt{1 - q^2\sin^2\psi}} = \frac{2n}{\pi}K(q). \tag{49}$$

From Eq. (49) it follows that for a given q value a corresponding P/P_E can directly be calculated, i.e. no iterations are needed, allowing the load–displacement curve to be drawn directly. It can be found from tables and graphs that $K(q)$ takes its minimum value $\pi/2$ for $q = 0$, showing that it will not be possible to find a deformed equilibrium for the column when $P < P_E$. The postbuckling behaviour for the classical inextensible elastica is shown in Fig. 4. Notice that, since the two end-points may come arbitrarily close to each other, and indeed even pass each other, the maximal deflection may in fact decrease with increasing load beyond the critical point.

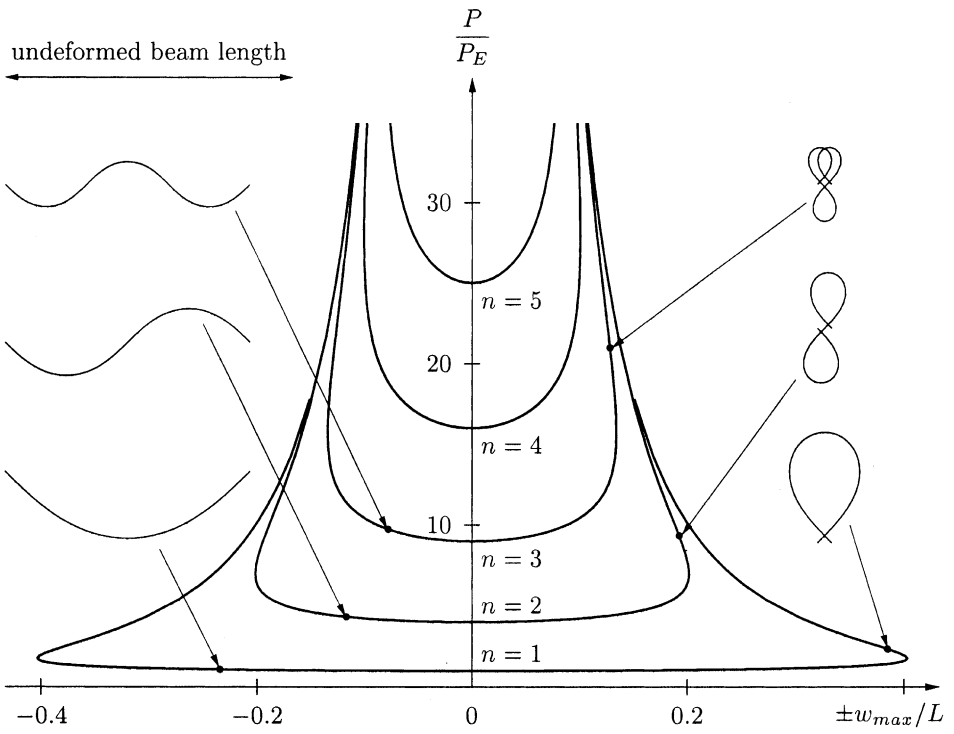

Fig. 4. Buckling behaviour of the classical inextensible elastica for the first five modes with the deformed shape for the first three modes. The upper left corner shows the undeformed beam.

Depending on the slenderness, different postbuckling behaviour is obtained for the extensible beam. As an example, for $\lambda = 6\pi$, Fig. 5 displays several instability phenomena. For mode 3, a double root is obtained at the fundamental path corresponding to point $B^{(2)}$ if Fig. 3, which can be seen since there are two paths emanating from the singular point, cf. Eq. (27) and Fig. 3. One of the difficulties with detecting higher order singularities are their sensitivity to imperfections. This can be seen in Fig. 6 where a small change in slenderness turns the double root into either two simple bifurcations for $\lambda = 6.05\pi$, or two nonbifurcating branches for $\lambda = 5.95\pi$. Moreover, for $n = 4$, a nonbifurcating branch is obtained, cf. Antman and Pierce (1990). Using an ordinary path following method in a finite element context, starting from zero load, this branch would never be detected, i.e. there exists a challenging problem in the numerical treatment. The isola bifurcation found by Antman and Pierce (1990) will not be found here, and is due to the linearity of the constitutive relation.

When the extensible elastica is used, it can be observed that the elastica can have postbuckling branches where the load initially decreases, see the lower branch in Fig. 6(a). The buckling behaviour goes from increasing load to decreasing load when the curvature of $P(q)$ changes sign around $q = 0$, i.e. when $(\mathrm{d}^2P/\mathrm{d}q^2 = 0)$. To find the value of λ where this occurs, use can be made of the analysis in Section 4.1. It was found that the critical load and slenderness where the curvature changes sign is given by Eq. (32), these events are marked by the points $A^{(i)}$ in Fig. 3.

At the secondary branches emerging from the fundamental path, an initial increase in load will be obtained for higher values of $\lambda > \lambda_{\mathrm{cr}}$, cf. also the discussion related to Eq. (32), whereas, an initial decrease in load will be obtained for lower vales of $\lambda < \lambda_{\mathrm{cr}}$. This means that the nth postbuckling branch displays an initial decrease in load for slenderness in the interval $2n\pi < \lambda < 4n\pi/\sqrt{3}$. These intervals, denoted by

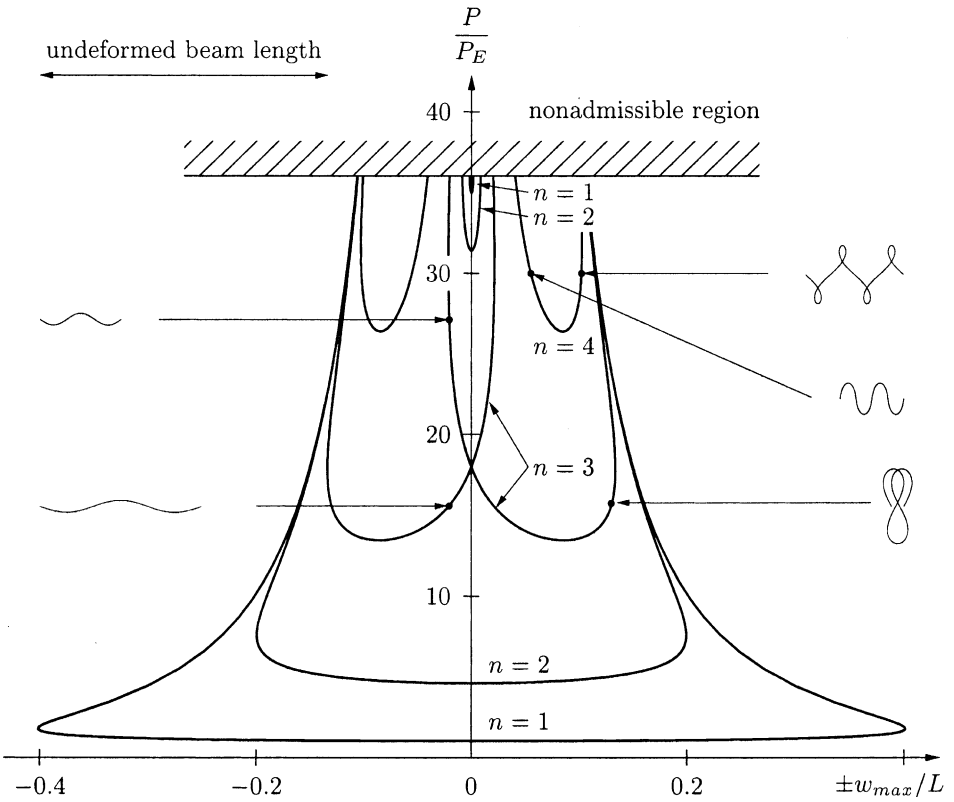

Fig. 5. Buckling behaviour for $\lambda = 6\pi$ where the deformed shape of the beam is shown. The upper left corner shows the undeformed beam.

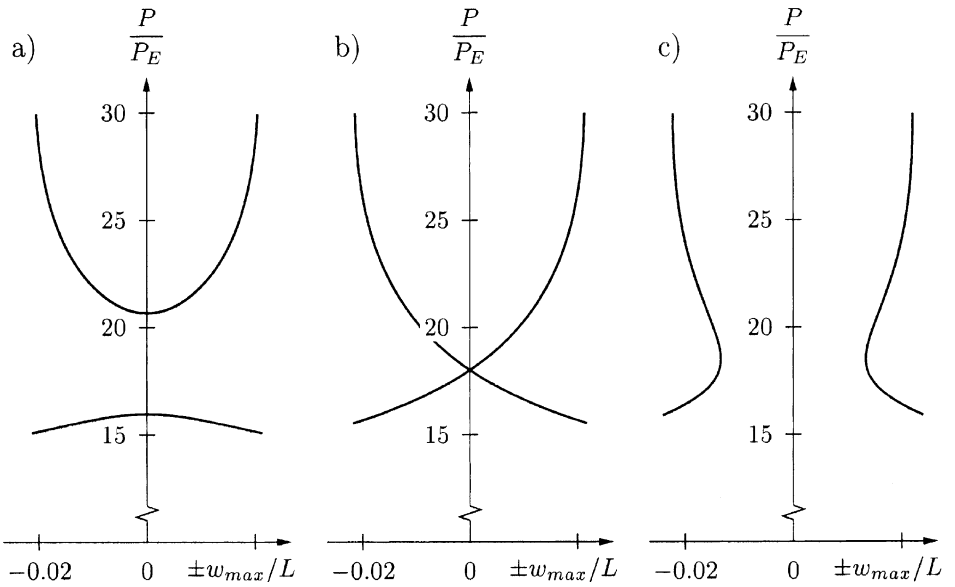

Fig. 6. Buckling behaviour for the third mode for (a) $\lambda = 6.05\pi$, (b) $\lambda = 6\pi$, and (c) $\lambda = 5.95\pi$.

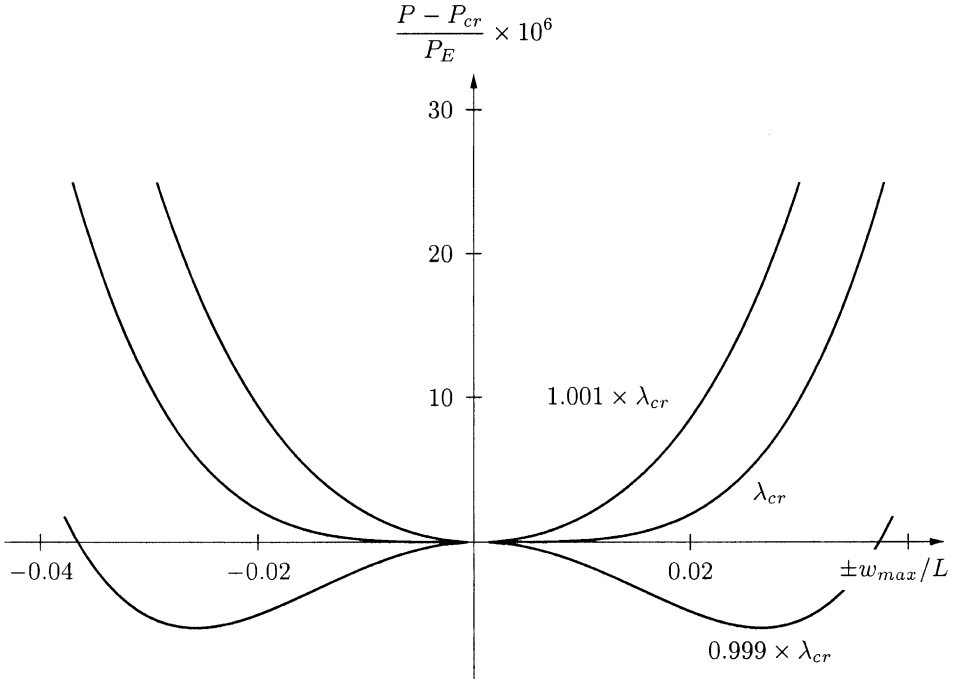

Fig. 7. Bifurcated paths for stable, critical and unstable elastica, where $\lambda_{cr} = (4/\sqrt{3})\pi$.

$A^{(n)} - B^{(n)}$, are shown in Fig. 3. For the first mode, this means that the behaviour of the bifurcation changes from supercritical to subcritical at the slenderness $\lambda = \lambda_{cr} = 4\pi/\sqrt{3}$. For $\lambda < 2\pi$ no buckling will occur and the fundamental solution is always stable, cf. Fig. 3. The discussion above is related to the lowest buckling load for a given mode, cf. Eq. (27). For the higher buckling load it turns out that the load on the secondary branches is increasing for all values of the slenderness λ, this was also concluded when the normal forms of the bifurcation points where discussed.

In Fig. 6(a) the slenderness is slightly higher than that of point $B^{(3)}$ in Fig. 3. The lower buckling load is in the interval $A^{(3)}$–$B^{(3)}$ where the load drops on the bifurcated paths. The higher buckling load is outside the interval $A^{(3)}$–$B^{(3)}$ and, thus has increasing load on the bifurcated paths. In Fig. 6(b) the slenderness is such that the buckling load for mode 3 is given by point $B^{(3)}$ in Fig. 3, corresponding to a double root, and in Fig. 6(c) the slenderness is slightly lower than that of point $B^{(3)}$, leading to two nonbifurcating branch.

In Fig. 7 the initial postbuckling response is plotted for $n = 1$, for values of the slenderness just above and just below the critical value as well as for the critical value $\lambda_{cr} = 4\pi/\sqrt{3}$. For clarity the load $(P_{cr}/P_E)_0$, which is the load at $w_{max} = 0$, has been subtracted from the total load P/P_E. This clearly shows the transition of the singularity from a supercritical to a subcritical bifurcation as the slenderness passes the critical value for the first mode.

5. Conclusions

To allow for the derivation of the extensible elastica solution use was made of the virtual work expression in which the Euler–Bernoulli assumption together with the definition of the nominal (Biot) strains was used; from this a kinematically exact beam theory could be derived. The differential equation suitable

for the axially loaded beam was then found by assuming a linear relationship between Biot's stress and the nominal (Biot) strain.

From the elastica solution several interesting observations could be made: The critical (bifurcation) load depends on the slenderness of the beam, but what is more interesting is that the usual supercritical bifurcation point, which always hold for the classical elastic solution of inextensible beam axis, becomes a subcritical bifurcation for small slenderness. The implication of this is that the bifurcation point per definition becomes unstable. Moreover, there are examples where two different postbuckling paths emerges from the fundamental path. Also nonbifurcating (isolated) branches could be found.

References

Abramowitz, M., Stegun, I. (Eds.), 1970. Handbook of Mathematical Functions With Formulas, Graphs and Mathematical Tables, ninth printing. Applied Mathematics Series 55, National Bureau of Standards.

Antman, S.S., 1972. The theory of rods. In: Flügge, S. (Ed.), Handbuch der Physik, vol. VIa/2, Springer, Berlin, pp. 641–703.

Antman, S.S., Pierce, J.F., 1990. The intricate global structure of buckled states of compressible columns. SIAM J. Appl. Math. 50 (2), 395–419.

Antman, S.S., Rosenfeld, G., 1978. Global behaviour of buckled states of nonlinearly elastic rods. SIAM Rev. 20 (3), 513–566; corrections and additions SIAM Rev. 22, 1980, pp. 186–187.

Atluri, S.N., Cazzani, A., 1995. Rotations in computational solid mechanics. Arch. Comput. Meth. Engng. 2 (1), 49–138.

Golubitsky, M., Schaeffer, D.G., 1984. Singularities and Groups in Bifurcation Theory, vol. I. Applied Mathematical Sciences 51, Springer.

Goto, Y., Yamashita, T., Matsurra, S., 1987. Elliptic integral solutions for extensional elastica with constant initial curvature. Struct. Engng./Earthquake Engng. 4 (2), 299–309.

Goto, Y., Yoshimitshu, T., Obata, M., 1990. Elliptic integral solutions of plane elastica with axial and shear deformations. Int. J. Solids Struct. 26 (4), 375–390.

Gröbner, W., Hofreiter, N., 1961. Integraltafel. Erster Teil, Unbestimmte Integrale. Springer, Wien.

Love, A.E.H., 1927. A Treatise on the Mathematical Theory of Elasticity, fourth ed. Cambridge University Press.

Pflüger, A., 1964. Stablilitätsprobleme der Elastostatik. Springer.

Poston, T., Stewart, I., 1996. Catastrophe Theory and Its Applications. Dover publications, Inc.

Reiss, E.L., 1969. Column buckling – an elementary example of bifurcation. In: Keller, J., Antman, S.S. (Eds.), Bifurcation theory and nonlinear eigenvalue problems. W.A. Benjamin, New York, pp. 1–16.

Reissner, E., 1972. On one-dimensional finite-strain beam theory: the plane problem. J. Appl. Math. Phys. 23, 795–804.

Reissner, E., 1973. On one-dimensional large-displacement finite-strain beam theory. Studies Appl. Math. LII (2), 87–95.

Reissner, E., 1981. On finite deformations of space-curved beams. J. Appl. Math. Phys. 32, 734–744.

Simo, J.C., 1985. A finite strain beam formulation – the three-dimensional dynamic problem part I. Comput. Meth. Appl. Mech. Engng. 49, 55–70.

Simo, J.C., Vu-Quoc, L., 1986. A three-dimensional finite-strain rod model. Part II: computational aspects. Comput. Meth. Appl. Mech. Engng. 58, 79–116.

Timoshenko, S.P., Gere, J.M., 1961. Theory of Elastic Stability, second ed. McGraw-Hill.

Troger, H., Steindl, A., 1991. Nonlinear Stability and Bifurcation Theory. Springer, Wien.

Truesdell, C., 1960. The rational mechanics of flexible or elastic bodies. L. Euleri Opera Omnia 11(Series 2) (2), 1638–1788.